

Experimental and Numerical Investigations on Flexural Behavior of Macro-Synthetic FRC

Ashkan Shafee, Ahamd Fahimifar, Sajjad V. Maghvan

Abstract—Promotion of the Fiber Reinforced Concrete (FRC) as a construction material for civil engineering projects has invoked numerous researchers to investigate their mechanical behavior. Even though there is satisfactory information about the effects of fiber type and length, concrete mixture, casting type and other variables on the strength and deformability parameters of FRC, the numerical modeling of such materials still needs research attention. The focus of this study is to investigate the feasibility of Concrete Damaged Plasticity (CDP) model in prediction of Macro-synthetic FRC structures behavior. CDP model requires the tensile behavior of concrete to be well characterized. For this purpose, a series of uniaxial direct tension and four point bending tests were conducted on the notched specimens to define bilinear tension softening (post-peak tension stress-strain) behavior. With these parameters obtained, the flexural behavior of macro-synthetic FRC beams were modeled and the results showed a good agreement with the experimental measurements.

Keywords—Concrete damaged plasticity, fiber reinforced concrete, finite element modeling, macro-synthetic fibers, direct tensile test.

I. INTRODUCTION

FIBER Reinforced Concrete (FRC) is the concrete containing different fibrous material such as steel, synthetic and glass. The fiber increases the ductility and integrity of concrete [1]. FRC is commonly used in different concrete applications (e.g., slabs, shotcrete in tunnels, precast concrete, tunnel segments, etc.). Studies show that fibers drastically improve the post-peak behavior of concrete, especially in tension and bending, preventing them from brittle failure and providing residual strength. Usually steel fibers are used for reinforcement purposes and micro-synthetic fibers are used for reducing shrinkage cracking, however, around the millennium, the producers of micro-synthetic fibers started to offer new high performance macro-synthetic fibers which gave the concrete the same toughness as steel fiber reinforced concrete [2].

Macro-synthetic fibers have low Young's modulus, ranging between 2 to 10 GPa, but very high failure strains up to 15%. As well as the mechanical properties, synthetic fibers are also resistant in corrosive environments and in overall cheaper than steel fibers. Macro-synthetic FRC can sustain relatively large loads despite cracking with large deflections and for this reason they are suitable for applications such as shotcreting in

tunnels.

There are numerous researches concerning the effects of fibers on mechanical behavior of concrete. Hsie et al. [3] tested the flexural behavior of macro-synthetic polypropylene FRC with the four-point beam-bending test. The fibers had diameter of 1 mm, length of 60 mm and Young's modulus of 5.88 GPa. They concluded that macro-synthetic fibers, at a dosage rate of 9 kg/m³, slightly improve the module of rupture and provide the residual flexural strength of around 1.5 MPa.

Reference [4] is a good comparative evaluation of steel mesh, steel and macro-synthetic fiber reinforced shotcrete. They used EFNARC panel tests on shotcrete panels containing different reinforcement and concluded that polypropylene macro-synthetic fiber reinforced shotcrete (FRS) had almost the same toughness performance as steel FRS at relatively low dosages of fiber.

Despite the numerous studies available about mechanical behavior of FRC, there has been little work done on numerical modeling of these materials. Sorelli et al. [5] investigated the application of non-linear fracture mechanics based on discrete crack approach for predicting the flexural behavior of simple and hybrid FRC. The procedure was to define the tensile post cracking law (post-peak tensile-crack opening displacement) through the simulation of the uniaxial tensile tests and subsequently to use the same law for simulating bending tests. Their numerical analysis results for bending tests was in a good agreement with the experimental data.

This study presents the results of an experimental and numerical investigations on the flexural behavior of macro-synthetic FRC beams with different dosages of fiber. The mixing proportions of cementitious materials and the aggregate matrix were chosen to be similar to a typical shotcrete mixture because of the fast growing interest in the use of macro-synthetic fibers in shotcrete application. The experiments involved four point beam bending tests on notched and un-notched specimens and uniaxial compressive and direct tensile tests to determine the parameters required for numerical modeling. In this study, since the aim was to capture the material behavior up to and past the peak loading, Concrete Damaged Plasticity model (CDP) was applied.

II. EXPERIMENTS

A. Materials

Fibers used in this study are Macro-synthetic wave-shaped monofilaments with the length of 35 mm, diameter of 0.78mm and Young's modulus of 3.6 GPa. Mixing proportions of cementitious materials and the aggregate grading of concrete were similar to a typical shotcrete mixture which is listed in

A. Shafee (master student), A. Fahimifar (professor) and S.V. Maghvan (master student) are with the Civil and Environmental Engineering Department of Amirkabir University of Technology, Tehran, Iran (phone: +98 914 305 2174; e-mail: ashkan.shafi@aut.ac.ir, fahim@aut.ac.ir, svmaghvan-sf69@aut.ac.ir).

Table I. Fiber type and concrete mixture design selection were due to the fast growing interest in the use of macro-synthetic fibers in shotcrete application. Fibers were added to the concrete matrix in three different volume fractions as shown in Table II.

TABLE I
 CONCRETE MIXTURE

Cement (Kg/m ³)	Aggregates (Kg/m ³)	Water (Kg/m ³)	Superplasticizer (L/m ³)
400	1800	174	2

TABLE II
 FIBER COMBINATION FOR SPECIMENS

Material	Plain	M3.5-8	M3.5-12	M3.5-18
Fiber volume fraction (%)	0	0.8	1.2	1.8

B. Experimental Setup

The experiments involved four point bending, unconfined compressive and direct tensile tests which were conducted with the servo-controlled testing machine (DARTEC 9600). Cylindrical specimens having a diameter of 75 mm and the length of 150 mm were used for unconfined compressive tests. Uniaxial direct tensile tests with freely rotating plates were performed on cylindrical specimens having a diameter of 75 mm and the length of 150 mm that had a circumferential notch with a depth of 6 mm and the width of 3 mm. The notched specimens and test setup for direct tensile test is shown in Fig. 1.

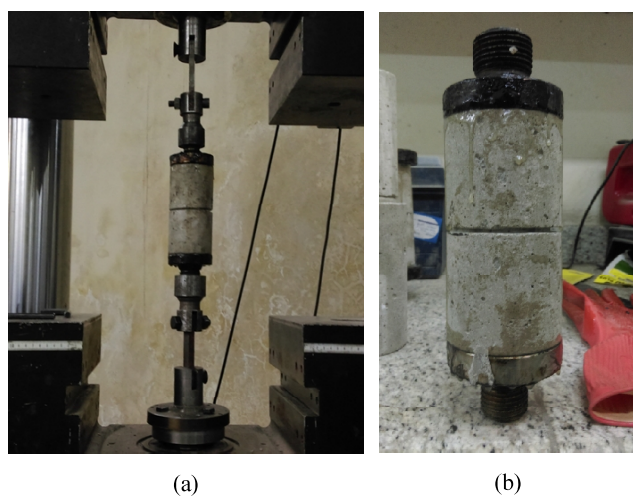


Fig. 1 (a) Direct Tensile test setup (b) Direct tensile test specimens glued to plates

Four point bending tests were performed on notched and un-notched beams having the size of 100×100×350 mm. The test procedure was according to ASTM C1609 and the notched beams had a central notch, with 20 mm depth and 3 mm width, which is illustrated in Fig. 2 [6].

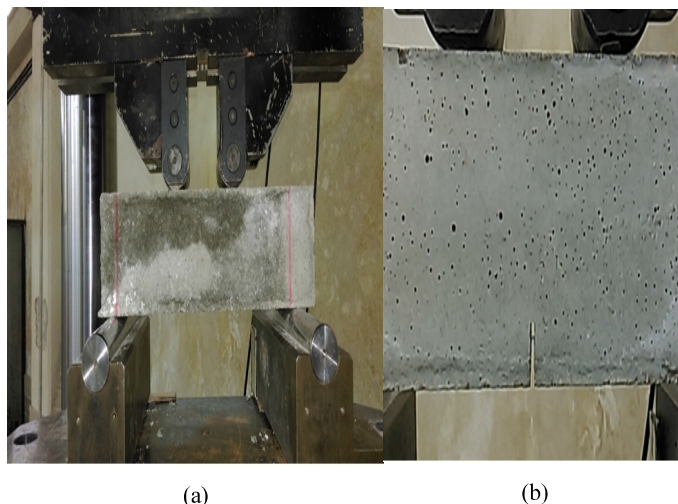


Fig. 2 (a) Four point bending test setup according to ASTM C1609
 (b) Geometry of a notched beam

III. RESULTS AND DISCUSSION

Results of unconfined compression tests are shown in in Fig. 3 as full compressive stress-strain diagrams which include two cycles of un-loading and re-loading in the post peak region. Compressive strength of concrete specimens was slightly improved with inclusion of fibers. This improvement is negligible and the average value for all specimens is 32 MPa. Also Young's modulus of specimens were calculated according to ASTM C469 which showed a negligible difference and so the average value of 13.32 GPa was selected [7].

Direct tensile tests on specimens having fibers with volume fraction of 0.8 % showed semi-brittle behavior which is due to insufficient area of fracture that does not include proper number of fibers. In addition to notched specimens, other direct tensile tests are conducted on un-notched plain specimens in order to obtain the tensile strength of concrete which was 3.15 MPa. Results of direct tensile tests are illustrated in Fig. 4 in terms of tensile force-deflection.

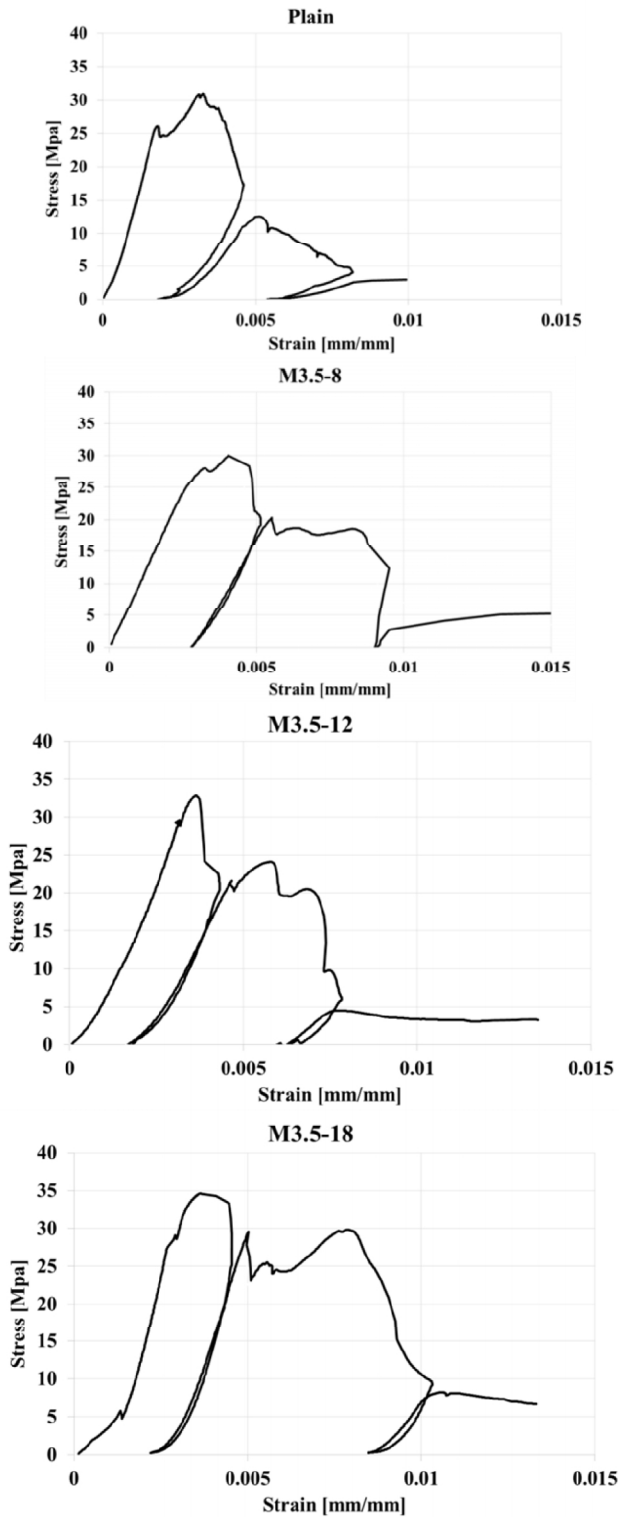


Fig. 3 Full compressive stress-strain diagrams

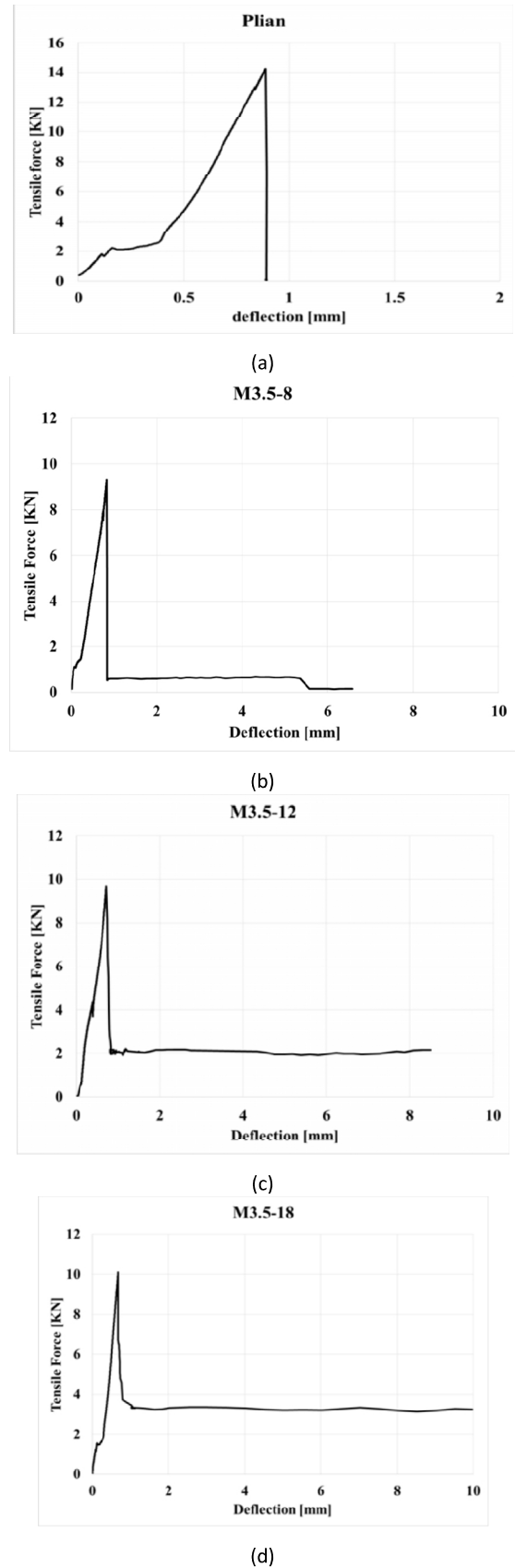


Fig. 4 (a) Un-notched plain concrete (b), (c), (d) direct tensile test on macro-synthetic FRC notched specimens

Results of four point bending tests on un-notched and notched beams are illustrated in Figs. 5 and 6, respectively. According to the results, un-notched beams showed elastic behavior until the failure point and then with the sudden drop of load bearing capacity to a residual amount.

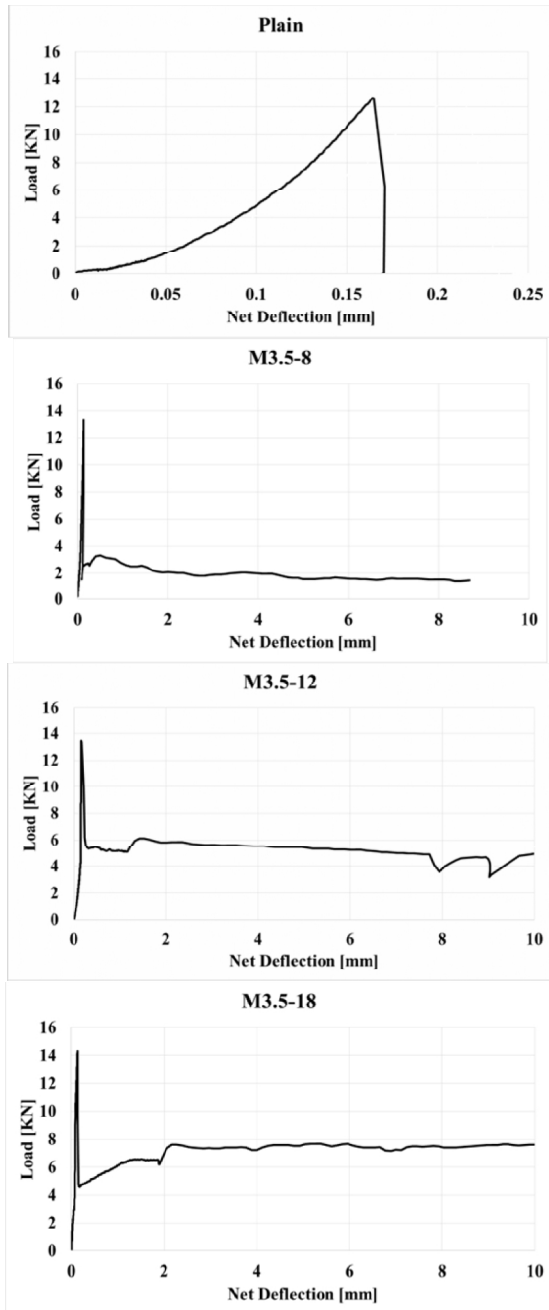


Fig. 5 Four point bending tests on un-notched beams according to ASTM C1609

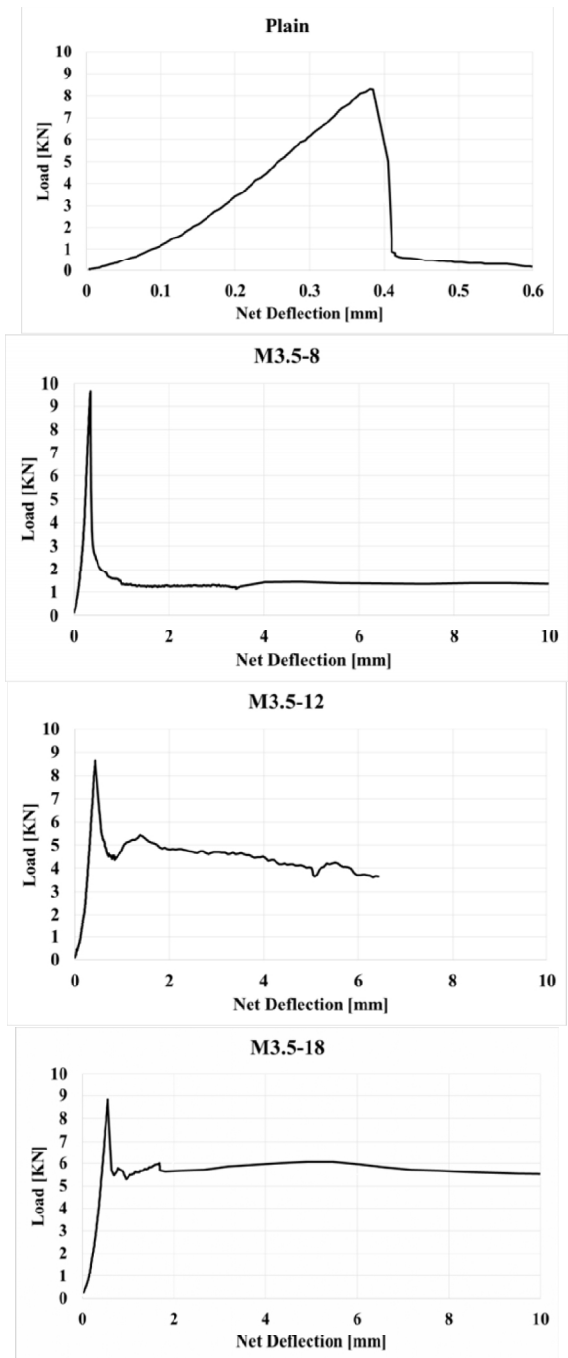


Fig. 6 Four point bending test on notched beams Numerical Modeling

The experiments were also numerically simulated with ABAQUS software utilizing Concrete Damaged Plasticity (CDP) model. CDP model requires compression and tensile behavior to be well characterized specifically in the post-peak zone. In this study, the procedure for obtaining post-peak tension behavior was to simulate the uniaxial tensile and four point bending tests on notched specimens (which are closer to the tensile behavior) and characterize the best fitted bilinear tension softening law for each material.

The uniaxial tensile test model was axisymmetric and the

elements used for this model were 3-node linear axisymmetric triangles. The approximate size of elements was 5 mm with few local refinement done in the notch zone. For the boundary conditions, at the bottom of model a pin was modeled and for the loading, prescribed displacement was presumed at top of model.

The four point bending test model was plane-stress and the elements used for this models was 3-node triangles as well. At one end of the beam a pin support was used and on the other end, the roller support was added as boundary conditions. The loading was simulated with prescribed displacement in one-thirds of loading span. Compressive strength and Young's modulus of specimens were assumed to be same for all specimens and were selected 34 MPa and 13.32 GPa, respectively. Also the Poisson's ratio was assumed to be 0.2 and other plasticity parameters were set to default values. Fig. 7 shows the models used for simulation uniaxial tensile and four point bending tests on notched specimens.

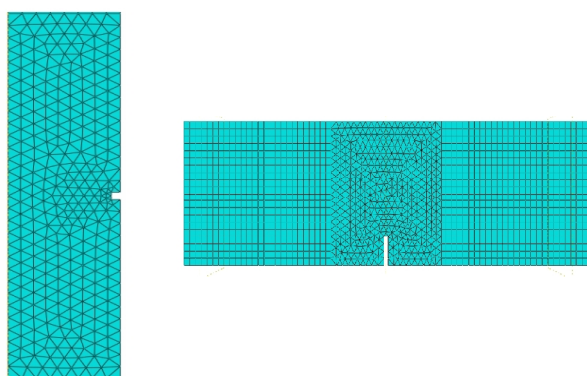


Fig. 7 Models used for simulation of uniaxial tensile and four point bending tests on notched specimens to define tension softening law

After a series of trial and error tests, the parameters of the bilinear tension softening law (post cracking tension stress-cracking strain) that provided the best fit for the uniaxial tensile and bending tests on notched specimens were obtained as summarized in Table III. In addition, the tension damage parameter was defined as 0 for un-cracked and 0.95 for total failure state to illustrate the crack path.

TABLE III
 TENSION SOFTENING LAW (POST-CRACKING TENSION STRESS VERSUS CRACKING STRAIN) AS AN INPUT DATA FOR CDP MODEL

	f_t (Mpa)	ϵ_{cr}	σ_{t1} (Mpa)	ϵ_{cr1}	σ_{t2} (Mpa)	ϵ_{cr2}
M3.5-18	3.15	0	2	10^{-7}	1	0.1
M3.5-12	3.15	0	1.5	10^{-7}	1	0.05
M3.5-8	3.15	0	1.2	10^{-7}	0.6	0.05

With tension softening laws obtained for each material, the four point flexural behavior of un-notched beams were simulated. The model for un-notched beam was plane-stress and boundary conditions and element types were the same as notched beams as discussed before. The comparison of the experimental measurements and the predicted data from

numerical modeling for load-deflection curves of each material are presented in Fig. 8. As can be seen, the numerical analysis utilizing CDP model shows a stiffer behavior up to failure and somewhat stronger response in the post-peak region up to 5 mm deflection but for larger deflections there is a good agreement between the experimental and numerical curves.

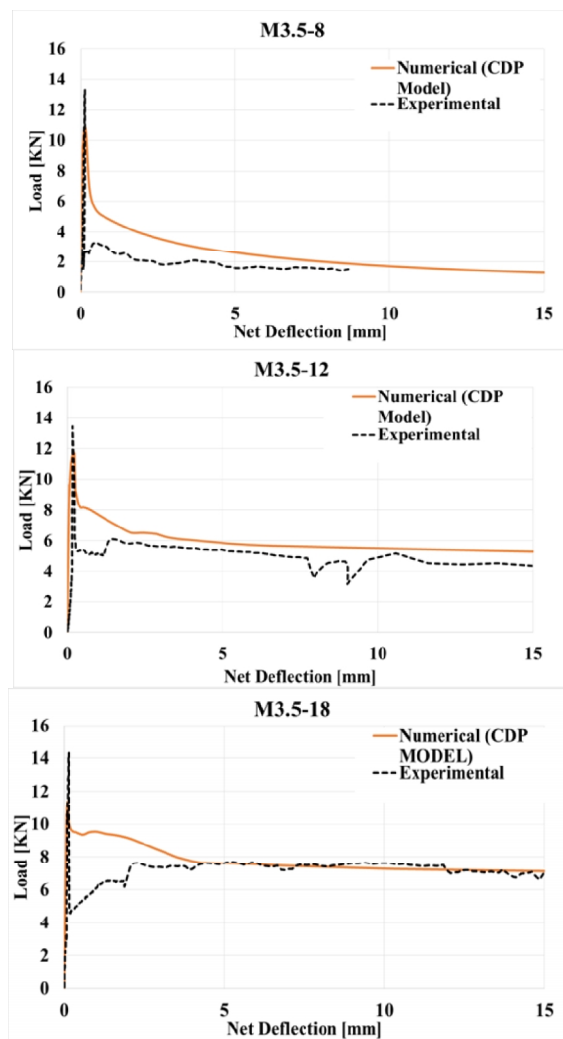


Fig. 7 Comparison of experimental and numerical (CDP model) results for net-deflection curves of each material

As mentioned before, the tension damage parameter is defined as 0 for un-cracked and 0.95 for fully failure state. Fig. 9 shows the tension damage contour with white and black presentation. As can be seen, the initiation and propagation of tension damage which presents the cracking path are well illustrated.

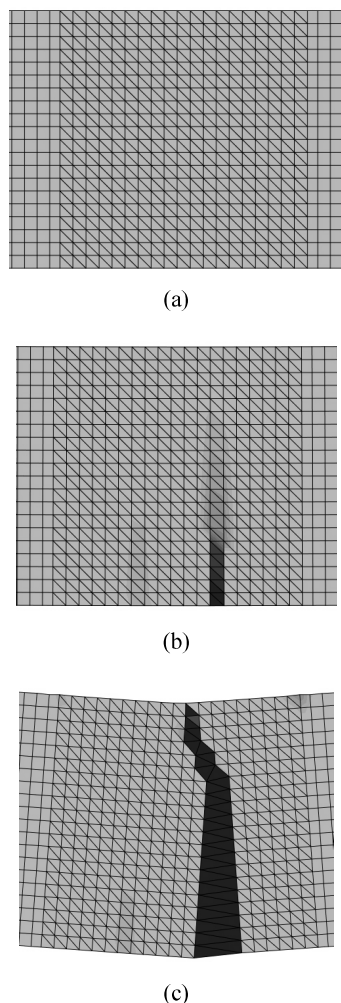


Fig. 9 Tension damage contour for mid-section of beam illustrating the crack path for (a) pre failure (b) initiation of failure (c) failed beam

IV. CONCLUSION

In the present work, the results of an unconfined compression, uniaxial direct tensile and four point bending on un-notched and notched beams on FRC specimens containing different dosages of fibers were presented. The main findings of the paper are summarized as following:

- Inclusion of macro-synthetic fibers does not show a considerable effect on compressive strength, however, generally speaking, causes the specimens show post-peak ductile behavior rather than brittle failure of plain concrete.
- Uniaxial direct tensile test on macro-synthetic FRC is hard to perform and the specimen geometry used in this study is not suitable because of insufficient area of fracture which does not include the representative number of fibers for each material.
- In the absence of reliable direct tensile test results, a series of four-point bending tests were conducted on notched beams to represent the pure tension behavior.

- The parameters of the bilinear tension softening law (post cracking tension stress-strain) which provided the best fit for the uniaxial tensile and bending tests on notched specimens were used in numerical modeling of un-notched beams.
- The predicted results of numerical analysis, utilizing CDP model, on the flexural behavior of un-notched macro-synthetic FRC beams showed a good agreement with the experimental data.
- CDP constitutive model can be used as an appropriate model for the analysis of macro-synthetic FRC structures, enabling the capture of the post-peak performance.

REFERENCES

- [1] Ronald F. Zollo. Fiber-reinforced Concrete: An Overview after 30 Years of Development. *Cement and Concrete Composites* 19 (1997) 107-122.
- [2] Ratcliffe R. Steel versus Synthetic Fiber Reinforcement in Shotcrete. Shotcrete for underground support. ASCE 2006
- [3] Hsie M, Tu C, Song PS. Mechanical properties of polypropylene hybrid fiberreinforced concrete. *Mat Sci Eng A Struct.* 2008;494(1-2):153-7
- [4] Cengiz O, Turanli L. Comparative evaluation of steel mesh, steel fibre and high-performance polypropylene fibre reinforced shotcrete in panel test. *Cement Concrete Res* 2004; 34(8):1357-64.
- [5] Sorelli L. G, Meda A, Plizzari G. A. Bending and Uniaxial Tensile Tests on Concrete Reinforced with Hybrid Steel Fibers. *J. Mater. Civ. Eng.* 2005.17:519-527.
- [6] ASTM Standards C1609/C1609M-12. 2012. Standard Test Method for Flexural Performance of Fiber-Reinforced Concrete (Using Beam with Third Point Loading). ASTM International,
- [7] ASTM Standards C469/C469-02. Standard Test Method for Static Modulus of Elasticity and Poisson's Ratio of Concrete in Compression. ASTM International